

Gold-Catalyzed Migratory Insertion of Alkynes

Avishek Das,[†] Biswajit Biswas,[†] Vincent Gandon,^{§*} and Nitin T. Patil^{†*}

[†]Department of Chemistry, Indian Institute of Science Education and Research Bhopal, Bhaeri, Bhopal 462 066, India

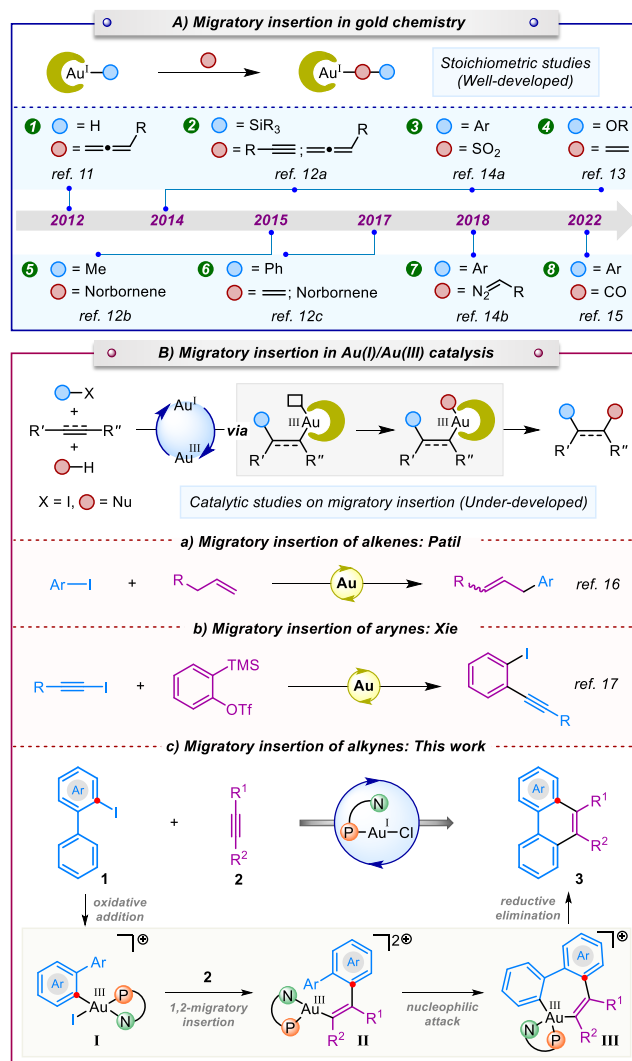
[§]Institut de Chimie Moléculaire et des Matériaux d'Orsay (UMR CNRS 8182), Paris-Saclay University, bâtiment Henri Moissan, 17 avenue des sciences, 91400 Orsay, France

Abstract: Herein, for the first time, we disclose the migratory insertion of alkynes into Au(III)–C bonds in a catalytic fashion. Experimental results clearly suggest that the migratory insertion pathway predominates over the π -activation pathway - a finding further supported by the Density Functional Theory (DFT) calculations. The observed regioselectivity underscores the distinct advantages and complementarity of gold catalysis in comparison to palladium catalysis.

Over the last two decades, gold catalysis has firmly established a prominent position in organic synthesis due to their soft π -acidic nature.¹ However, owing to the high redox potential of the Au(I)/Au(III) couple ($E^0 = +1.41$ V), gold does not readily undergo two-electron redox cycle.² Over the years, there has been significant advancement in the field of gold redox catalysis, largely centered on the following reactivity principles: a) employing external oxidants,³ b) utilizing aryl diazonium salts in combination with photocatalyst,⁴ c) employing EBX reagents,⁵ and d) utilizing electricity.⁶ Recently, the ligand-enabled Au(I)/Au(III) catalysis has evolved as a new technique, expanding the repertoire of gold redox catalysis. The potential of this strategy has been showcased for the development of various cross-coupling as well as 1,2-difunctionalization reactions of C–C multiple bonds.^{7,8}

Migratory insertion represents a crucial elementary process within organometallic chemistry, frequently encountered for most transition metals.⁹ However, in the realm of gold catalysis, the migratory insertion step remained elusive for a long time.¹⁰ As far as stoichiometric studies are concerned, there exist few reports on migratory insertion in gold chemistry (Scheme 1A). The migratory insertion of C–C multiple bonds into Au(I)–H, Au(I)–Si, Au(III)–O, Au(III)–C have been reported by the research group of Bochmann,¹¹ Amgoune/Bourissou,¹² and Tilstet,¹³ respectively. Further, Toste and co-workers demonstrated the migratory insertion of SO₂ and carbenes into Au(I)–C and Au(III)–C bonds, respectively.¹⁴ Bower/Russell and co-workers developed the migratory insertion of CO into the Au(III)–C bond in a stoichiometric manner.¹⁵ As far as catalytic versions are concerned, our group demonstrated the gold-catalyzed Heck reaction, which involves the sequence of migratory insertion/ β -H elimination in a catalytic fashion (Scheme 1Ba).¹⁶ Xie and co-workers reported the iodo-alkynylation reaction involving the gold-catalyzed migratory insertion of benzynes (Scheme 1Bb).¹⁷ Interestingly, there exists no report on the gold-catalyzed migratory insertion of alkynes.

We envisioned that the Au(III) complex **I**, generated after the oxidative addition of aryl iodide **1** with Me₂DalPhosAuCl, would undergo 1,2-migratory insertion with alkyne **2** to form vinyl Au(III) complex **II**. The vinyl Au(III) complex **II** would undergo intramolecular cyclization to form auracycle **III** which upon reductive elimination would afford the product **3** (Scheme 1Bc). The details of reaction development, substrate scope, and mechanistic studies have been reported herein. Experimental results combined with DFT calculations suggest that the migratory insertion pathway operates over the π -activation pathway, marking this work as the first example of the migratory insertion of alkynes into Au(III)–C bonds in a catalytic manner.

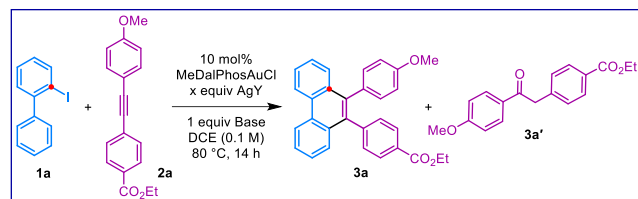


Scheme 1. Background and synopsis of present work

We initiated our investigation by using 2-iodo-1,1'-biphenyl **1a** (1.0 equiv) with ethyl 4-((4-methoxyphenyl)-ethynyl)benzoate **2a** (1.0 equiv) in the presence of Me₂DalPhosAuCl (10 mol%) and AgSbF₆ (1.1 equiv) in DCE (0.1 M) at 80 °C (Table 1). Unfortunately, we observed the formation of hydration product **3a'** as major (20% yield) along with the desired product **3a** in 12% yield (entry 1). The introduction of 1.0 equiv of K₂CO₃ improved the yield of **3a** up to 35%, while increasing its equivalence did not provide any better results (entries 2-3). Pleasingly, the formation of the hydration product was suppressed by increasing the equivalence of **1a** (entry 4-5). Further, the screening of silver salts re-

vealed a detrimental effect on the yield of the reaction (entries 6-7). Notably, the screening of bases and solvents (entries 8-12) revealed that using ^tBuONa as a base significantly improves the yield of **3a** up to 92% (entry 12). Further, lowering the reaction temperature to 40 °C led to a diminished yield (entry 13).

Table 1. Optimization of reaction conditions^[a,b]



| Entry | 1a (equiv) | AgY (x equiv) | Base (equiv) | % Yield | |
|-----------------------|----------------------|--------------------------------|-------------------------------------|-----------|------------|
| | | | | 3a | 3a' |
| 1 | 1 | AgSbF ₆ (1.1) | None | 12 | 20 |
| 2 | 1 | AgSbF ₆ (1.1) | K ₂ CO ₃ (1) | 35 | 25 |
| 3 | 1 | AgSbF ₆ (1.1) | K ₂ CO ₃ (2) | 35 | 23 |
| 4 | 1.5 | AgSbF ₆ (1.6) | K ₂ CO ₃ (1) | 42 | 18 |
| 5 | 2 | AgSbF ₆ (2.1) | K ₂ CO ₃ (1) | 65 | 10 |
| 6 | 2 | AgNTf ₂ (2.1) | K ₂ CO ₃ (1) | 57 | 15 |
| 7 | 2 | AgOTf (2.1) | K ₂ CO ₃ (1) | <5 | ND |
| 8 | 2 | AgSbF ₆ (2.1) | K ₃ PO ₄ (1) | 48 | 27 |
| 9 | 2 | AgSbF ₆ (2.1) | DTBP (1) | 10 | ND |
| 10 | 2 | AgSbF ₆ (2.1) | Cs ₂ CO ₃ (1) | 56 | 15 |
| 11 | 2 | AgSbF ₆ (2.1) | ^t BuONa (1) | 75 | 8 |
| 12^c | 2 | AgSbF₆ (2.1) | ^tBuONa (1) | 92 | 6 |
| 13 ^d | 2 | AgSbF ₆ (2.1) | ^t BuONa (1) | 70 | 15 |

^[a]Reaction conditions: 0.1 mmol **1a**, 0.1 mmol **2a**, 0.01 mmol MeDalPhosAuCl, 0.11 mmol AgSbF₆, DCE (0.1 M), 80 °C, 14 h. ^[b]Isolated yields. ^[c]DCM was used instead of DCE. ^[d]Reaction was performed at 40 °C for 24 h. ND = Not detected.

With the optimal reaction condition identified, we first explored the substrate scope of alkynes **2** by using 2-iodo-1,1'-biphenyl **1a** as a model substrate (Figure 1a). To our delight, various electronically biased internal alkynes **2** reacted efficiently under the optimized reaction conditions to afford the corresponding phenanthrene derivatives **3**. For instance, unsymmetrical diaryl alkynes containing 4-methoxyarene and different electron-deficient groups (-CO₂Et, -CO₂Me, -Ac, -NO₂, -CN, -Ms, -SO₂Ph, -CF₃, -F, -Ph) at the *para/meta* position of the other arene were well tolerated, providing **3a-3k** in good to excellent yields (51–92%). Next, the presence of weakly donating groups such as trifluoromethoxy and methyl groups at the aryl alkyne also afforded the corresponding products **3l-3m** in good yields (42–60%). Further, methyl 4-((3,4-dimethoxyphenyl)ethynyl)benzoate **2n** furnished the desired product **3n** in excellent yield (96%). Various unsymmetrical alkynes bearing electronically diverse substituents (**2o-2r**) worked well to deliver the products **3o-3r** in 45–76% yields. Notably, the present methodology is also suitable for symmetrical alkynes, generating the corresponding products **3s-3w**, in good to excellent yields (38–91%). Gratifyingly, alkynes containing various halo-substituents (-F, -Cl, -Br) were well toler-

ated under the standard reaction conditions to furnish the products **3x-3z** in moderate yields (53–57%). However, the symmetrical diaryl alkynes (**2aa-2ab**) bearing either electron-rich or electron-deficient group did not provide desired products. Next, 3,5-disubstituted diaryl alkyne **2ac** reacted smoothly to furnish the desired product **3ac** in 83% yield.

Next, we evaluated the scope of aryl iodides **1** using **2b** as an alkyne coupling partner (Figure 1b). In particular, aryl iodides bearing various electron-rich substituents at the *para* position delivered the products **3ad-3af** in 72–95% yields. The structure of product **3ae** was confirmed by X-ray crystallographic analysis.¹⁸ Electron-deficient aryl iodides **2ag** and **2ah** were found to furnish the products (**3ag-3ah**) in slightly lower yield (31–60%), while **2ai** failed to provide the desired product **3ai**. This observation aligns with our earlier result that electron-rich aryl iodides are required for migratory insertion in gold-catalyzed Heck reactions.¹⁶ Furthermore, aryl iodides having electron-rich, and halo substituents present at different positions of the pendant aryl ring reacted efficiently to afford the corresponding products **3ak-3ar** in good to excellent yields (46–81%).

Next, the usefulness of the method has been showed for the synthesis of polycyclic aromatic hydrocarbons (PAHs) (**4a-4d**) *via* the Scholl reaction (Figure 1c).¹⁹ Interestingly, when **3b** was subjected to Scholl reaction conditions, spiro-fused PAH **4e'** was obtained in 67% yield.

To shed light on the reaction mechanism, a few control experiments were performed (Figure 2). First, in order to investigate the effect of alkyne on the oxidative addition step, a stoichiometric reaction was carried out and monitored by ³¹P NMR spectroscopy (Figure 2a). We observed that, in the presence of electronically biased alkynes **2b**, complete oxidative addition of aryl iodide **1b** with MeDalPhosAuCl occurred after 30 min *via* the intermediacy of Au(I)-complex **IV**. This observation suggests the role of alkynes in hampering the rate of oxidative addition.^{8i,20} Further, the formation of putative Au(III) intermediates **I** (*m/z* = 928.2392) and **D** (*m/z* = 1066.4212) was also confirmed by mass spectrometric studies (Figure 2b).

Next, we questioned whether oxyarylation of alkynes could produce α -aryl ketones **5a**, which, upon condensation reaction, would afford the desired product **6ae** (Figure 2c). To check this possibility, when 4-iodoanisole **5b** and alkyne **2a** were subjected under standard conditions, we observed the formation of hydration product **3a'** in 52% yield, instead of α -aryl ketones **5c** (Figure 2d).²¹ Moreover, if this pathway is operational, regioisomer **6ae** would form. Since we did not observe the formation of **6ae**, the possibility of oxyarylation-condensation cascade has been ruled out.

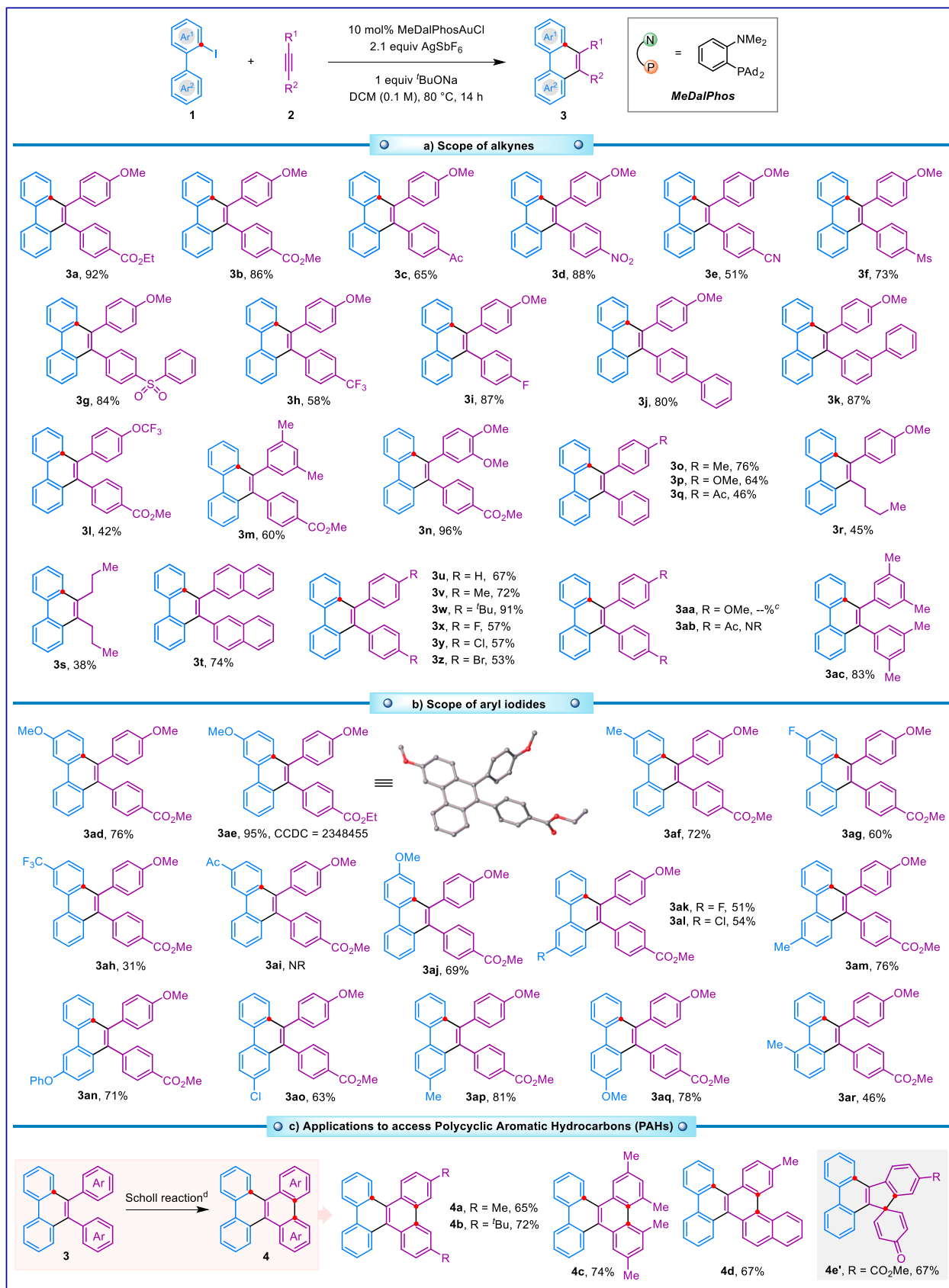


Figure 1. Scope of the reaction^[a,b]

^[a]Reaction conditions: 0.2 mmol **1a**, 0.1 mmol **2a**, 0.01 mmol MeDalPhosAuCl, 0.21 mmol AgSbF₆, 0.1 mmol ^tBuONa, DCM (0.1 M), 80 °C, 14 h.

^[b]Isolated yields. ^[c]Complex reaction mixture. NR = No reaction. ^[d]1 equiv **3**, 2 equiv DDQ, 10 equiv TfOH, DCM (0.021 M), 0 °C-rt, 5 min.

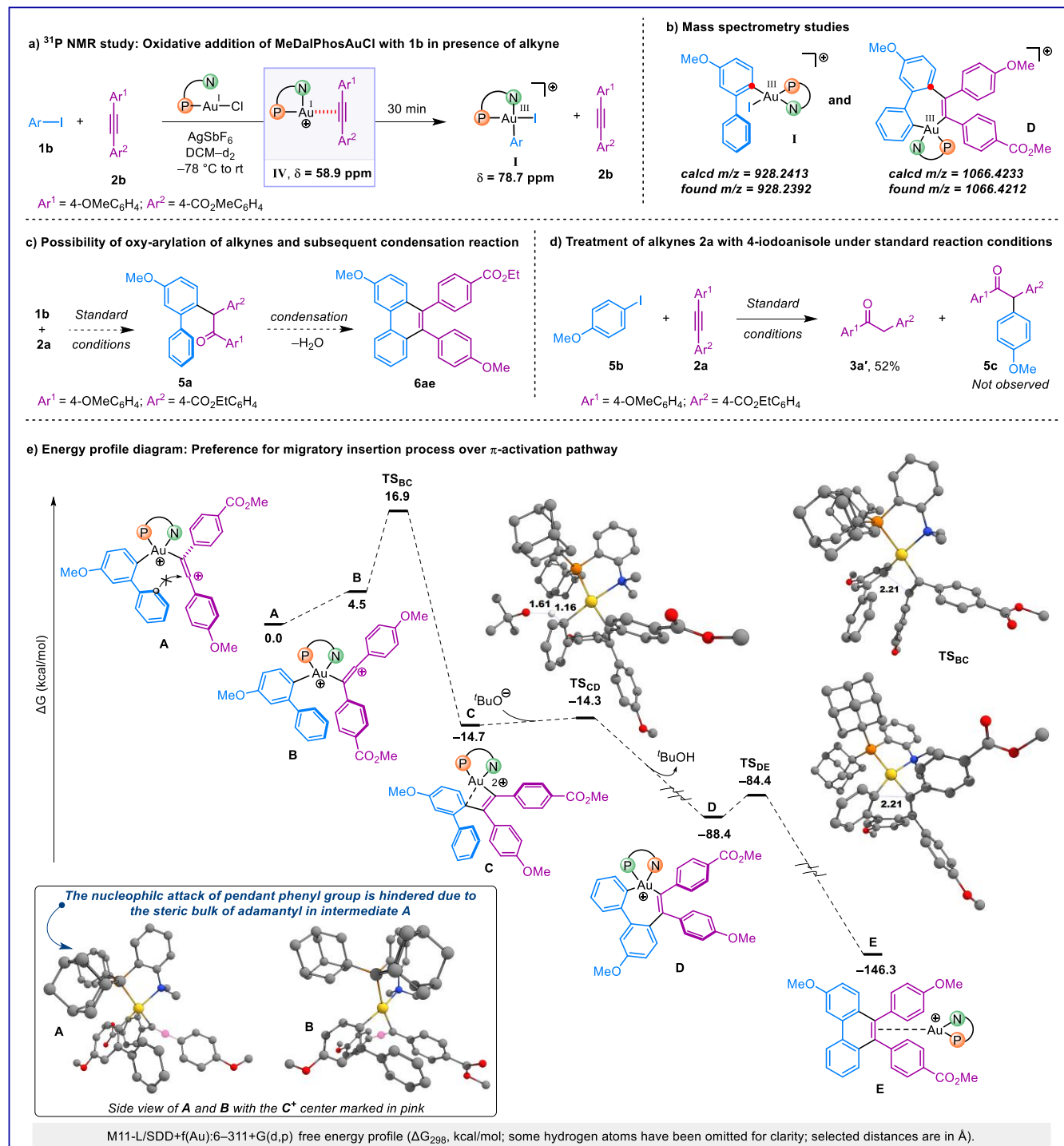


Figure 2. Mechanistic investigations

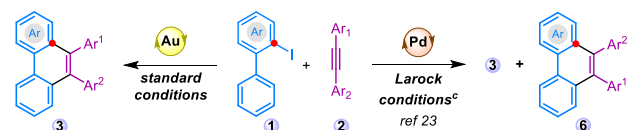
Based on the literature reports,^{8i,20} observed regioselectivity and control experiments, we propose the 1,2-migratory insertion pathway over the π -activation pathway (ESI, Section 8).²² Further, to get a deeper insight into the reaction mechanism, DFT computations were performed with the Gaussian 16 set of programs utilizing **1b** and **2b** as model substrates.²² The investigation started from the putative Au(III) alkyne complex **A**, which was used as reference of the free energies (Figure 2e). Due to the presence

of an electron-rich arene group at the alkyne moiety, this species converges as a vinyl carbocation on the *para*-methoxyphenyl side. A direct addition of the *ortho* carbon of the phenyl group (see grey dot in **A**) of the biphenyl core to the carbocation could not be modeled. A relaxed scan revealed an infinite rise of energy. Attempts were made to use a base during this approach ($^t\text{BuO}^-$) to assist the $\text{S}_{\text{E}}\text{Ar}$ process, but the steric bulk brought about by the adamantyl and *N*-methyl substituents prevented it (Figure 2e,

bottom left). In **A**, the *para*-methoxyphenyl group stabilizing the vinyl cation is oriented in the same direction as the phenyl group of the biphenyl moiety. It is, therefore, possible to define **B**, in which the methylbenzoate moiety is oriented towards this phenyl group. The latter is less stable by 4.5 kcal/mol. However, only **B** has the appropriate orientation to allow a 1,2-insertion process into the Au(III)–C_{Ar} bond (see side views, bottom left). The corresponding transition state, **TS_{BC}**, was located at 16.9 kcal/mol on the free energy surface. The resulting migratory insertion complex **C** (–14.7 kcal/mol) is formed in an appreciably exergonic fashion, the gold atom being coordinated by the biphenyl carbon *para* to the methoxy group. We then studied the auration of the *ortho* carbon of the phenyl group. Again, the approach of the phenyl group towards the gold center did not lead to a transition state, suggesting that a base is required. This time, enough space was found to use ^tBuO[–] during the approach of the phenyl group (see **TS_{CD}**). The resulting carboauration transition state **TS_{CD}** (–14.3 kcal/mol) was located 0.4 kcal/mol above **C**. After elimination of ^tBuOH, the cyclometallated complex **D** (–88.4 kcal/mol) is obtained in a markedly exergonic way. The reductive elimination was achieved through **TS_{DE}** (–84.4 kcal/mol), which is close in energy to **D**. This step benefits from a strong stabilization due to the aromatic character of the formed ring, providing complex **E** lying as low as –146.3 kcal/mol on the free energy surface. Overall, the mechanism presented in Figure 2e is energetically feasible and rationalizes the observed regioselectivity. Another set of computations using **1a** and 2-butyne as model unbiased alkyne was also performed.²²

Next, we conducted comparative studies between gold catalysis approach with Larock's palladium-catalyzed reaction²³ to understand regioselectivity differences (Scheme 2). Interestingly, under palladium catalysis, a mixture of regioisomers (**3ae** + **6ae**, **3as** + **6as**, **3at** + **6at**, **3au** + **6au**, and **3ad** + **6ad**) was obtained; whereas, gold catalysed reactions provided a single regioisomer (**3ae**, **3as**, **3at**, **3au** and **3ad**). The observed regioselectivity in gold catalysis can be attributed to the high carbophilic nature of Au(III) species, which polarizes the alkyne and distinguishes between the two C(sp)-centers.

In conclusion, we report the first example of the migratory insertion of alkynes into Au(III)–C bonds in a catalytic manner. Experimental results combined with DFT calculations suggest that the migratory insertion pathway operates over the π -activation pathway. The utility of the products has been demonstrated for the synthesis of various PAHs *via* Scholl reaction. Given the pivotal role of alkyne migratory insertion in organic synthesis,⁹ and the fact that gold exhibits complementary reactivity as compared to other transition metal catalysts,^{8b,8g,20b,24} we foresee tremendous development in the field.



| Entry | 3 and 6 | Au | Pd |
|-------|---|-------------------|--|
| 1 | 3ae , CCDC = 2348455 6ae | 3ae 95% | (3ae + 6ae) 56% ^d (3ae : 6ae) = 3:1 (inseparable) |
| 2 | 3as , CCDC = 2348456 6as | 3as 68% | (3as + 6as) 53% ^d (3as : 6as) = 2:1 (inseparable) |
| 3 | 3at 6at | 3at 60% | (3at + 6at) 51% ^d (3at : 6at) = 1:1 (inseparable) |
| 4 | 3au 6au | 3au 80% | (3au + 6au) 51% ^d (3au : 6au) = 3:1 (inseparable) |
| 5 | 3ad 6ad | 3ad 72% | (3ad + 6ad) 45% ^d (3ad : 6ad) = 4:1 (inseparable) |

Scheme 2. Observed regioselectivity: gold vs palladium catalysis^[a,b]

^[a]Reactions conditions: 0.2 mmol **1a**, 0.1 mmol **2a**, 0.1 mmol MeDalPhosAuCl, 0.21 mmol AgSbF₆, 0.1 mmol ^tBuONa, DCM (0.1 M), 80 °C, 14 h. ^[b]Isolated yields. ^[c]Larock conditions: 0.1 mmol **1a**, 0.11 mmol **2a**, 0.005 mmol Pd(OAc)₂, 0.2 mmol NaOAc, 0.1 mmol LiCl, DMF (0.1 M), 100 °C, 24 h. ^[d]Combined yields.

Acknowledgment

Generous financial support by the Science and Engineering Research Board (SERB), New Delhi (File Nos. CRG/2022/000195, SCP/2022/000063, and JCB/2022/000052) is gratefully acknowledged. A.D. thanks IISER Bhopal and SERB, B.B. thanks UGC for fellowships. V.G. thanks CNRS and UPSaclay for financial support. This work was granted access to the HPC resources of CINES under the allocation 2020-A0070810977 made by GENCI.

References

- [1] Books: (a) *Catalysis by Gold*; Catalytic Science Series: Vol. 6, Eds.: G. C. Bond, C. Louis and D. T. Thompson, Imperial College Press, London, 2006. (b) *Modern Gold Catalyzed Synthesis*; Eds.: A. S. K. Hashmi and F. D. Toste, Wiley-VCH, Weinheim, 2012. (c) *Gold Catalysis: An Homogeneous Approach*; Vol. 13, Eds.: F. D. Toste and V.

- Michelet, Imperial College Press, London, 2014. (d) Homogeneous Gold Catalysis; Vol. 357, Eds.: L. M. Slaughter, Springer International, Berlin, 2015. (e) A. G. Tathe, V. W. Bhoyare, N. T. Patil, Gold Dual Catalysis with Palladium, Nickel, or Rhodium, Science of Synthesis: Dual Catalysis in Organic Synthesis 1, G. Molander Thieme, Stuttgart, 2020.
- [2] S. G. Bratsch, *J. Phys. Chem. Ref. Data* 1989, 18, 1-21.
- [3] Reviews: (a) J. Miró, C. del Pozo, *Chem. Rev.* 2016, 116, 11924-11966. (b) A. Nijamudheen, A. Datta, *Chem. Eur. J.* 2020, 26, 1442-1487.
- [4] Reviews: (a) M. N. Hopkinson, A. Tlahuext-Aca, F. Glorius, *Acc. Chem. Res.* 2016, 49, 2261-2272. (b) M. O. Akram, S. Banerjee, S. S. Saswade, V. Bedi, N. T. Patil, *Chem. Commun.* 2018, 54, 11069-11083. (c) S. Witzel, A. S. K. Hashmi, J. Xie, *Chem. Rev.* 2021, 121, 8868-8925.
- [5] Review: S. Banerjee, V. W. Bhoyare, N. T. Patil, *Chem. Commun.* 2020, 56, 2677-2690.
- [6] Review: (a) A. Kumar, N. Bhattacharya, N. T. Patil, *ChemCatChem* 2024, DOI: 10.1002/cctc.202401112. Selected reports: (b) X. Ye, P. Zhao, S. Zhang, Y. Zhang, Q. Wang, C. Shan, L. Wojtas, H. Guo, H. Chen, X. Shi, *Angew. Chem. Int. Ed.* 2019, 58, 17226-17230. (c) A. Kumar, K. Shukla, S. Ahsan, A. Paul, N. T. Patil, *Angew. Chem. Int. Ed.* 2023, 62, e202308636. (d) H. Liang, Y. Julaiti, C.-G. Zhao, J. Xie, *Nat. Synth.* 2023, 2, 338-347.
- [7] Reviews: (a) B. Huang, M. Hu, F. D. Toste, *Trends Chem.* 2020, 2, 707-720. (b) C. Fricke, W. B. Reid, F. A. Schoenebeck, *Eur. J. Org. Chem.* 2020, 2020, 7119-7130. (c) P. Font, X. Ribas, *Eur. J. Inorg. Chem.* 2021, 2021, 2556-2569. (d) V. W. Bhoyare, A. G. Tathe, A. Das, C. C. Chintawar, N. T. Patil, *Chem. Soc. Rev.* 2021, 50, 10422-10450. (e) S. B. Ambegave, N. T. Patil, *Synlett* 2023, 34, 698-708. (f) P. Font, H. Valdés, X. Ribas, *Angew. Chem. Int. Ed.* 2024, 63, e202405824.
- [8] Selected reports: (a) A. Zeineddine, L. Estevez, S. Mallet-Ladeira, K. Miqueu, A. Amgoune, D. Bourissou, *Nat. Commun.* 2017, 8, 565. (b) J. Rodriguez, A. Zeineddine, E. D. Sosa Carrizo, K. Miqueu, N. Saffon-Merceron, A. Amgoune, D. Bourissou, *Chem. Sci.* 2019, 10, 7183-7192. (c) M. O. Akram, A. Das, I. Chakrabarty, N. T. Patil, *Org. Lett.* 2019, 21, 8101-8105. (d) J. Rodriguez, N. Adet, N. Saffon-Merceron, D. Bourissou, *Chem. Commun.* 2020, 56, 94-97. (e) S. R. Mudshinge, Y. Yang, B. Xu, G. B. Hammond, Z. Lu, *Angew. Chem. Int. Ed.* 2022, 61, e202115687. (f) P. Font, H. Valdés, G. Guisado-Barrios, X. Ribas, *Chem. Sci.* 2022, 13, 9351-9360. (g) A. Das, N. T. Patil, *ACS Catal.* 2023, 13, 3847-3853. (h) Urvashi; S. Mishra, N. T. Patil, *Chem. Sci.* 2023, 14, 13134-13139. (i) S. P. Sancheti, Y. Singh, M. V. Mane, N. T. Patil, *Angew. Chem. Int. Ed.* 2023, 62, e202310493. (j) P. Gao, J. Xu, T. Zhou, Y. Liu, E. Bisz, B. Dziuk, R. Lalancette, R. Szostak, D. Zhang, M. Szostak, *Angew. Chem. Int. Ed.* 2023, 62, e202218427. (k) S. C. Scott, J. A. Cadge, G. K. Boden, J. F. Bower, C. A. Russell, *Angew. Chem. Int. Ed.* 2023, 62, e202301526. (l) W. Li, Y. Chen, Y. Chen, S. Xia, W. Chang, C. Zhu, K. N. Houk, Y. Liang, J. Xie, *J. Am. Chem. Soc.* 2023, 145, 14865-14873. (m) K. Muratov, E. Zaripov, M. V. Berezovski, F. Gagosz, *J. Am. Chem. Soc.* 2024, 146, 3660-3674. (n) B. Paroi, C. Pegu, M. V. Mane, N. T. Patil, *Angew. Chem. Int. Ed.* 2024, DOI: 10.1002/anie.202406936. (o) J. Wu, W. Du, L. Zhang, G. Li, R. Yang, Z. Xia, *JACS Au*, 2024, DOI: 10.1021/jacsau.4c00422.
- [9] Books: a) R. H. Crabtree, *The Organometallic Chemistry of the Transition Metals*, 4th, Wiley, Hoboken, 2005. (b) J. F. Hartwig, *Organotransition Metal Chemistry From Bonding to Catalysis*, University Science Books, Sausalito, 2010. (c) D. M. P. Mingos, R. H. Crabtree, *Comprehensive Organometallic Chemistry III*, Elsevier, 2007, 269-314. Review: K. J. Cavell, *Coord. Chem. Rev.* 1996, 155, 209-243.
- [10] Review: M. Joost, A. Amgoune, D. Bourissou, *Angew. Chem. Int. Ed.* 2015, 54, 15022-15045.
- [11] D.-A. Roşca, D. A. Smith, D. L. Hughes, M. Bochmann, *Angew. Chem. Int. Ed.* 2012, 51, 10643-10646.
- [12] (a) M. Joost, L. Estevez, S. Mallet-Ladeira, K. Miqueu, A. Amgoune, D. Bourissou, *J. Am. Chem. Soc.* 2014, 136, 10373-10382. (b) F. Rekhroukh, R. Brousses, A. Amgoune, D. Bourissou, *Angew. Chem. Int. Ed.* 2015, 54, 1266-1269. (c) F. Rekhroukh, C. Blons, L. Estévez, S. Mallet-Ladeira, K. Miqueu, A. Amgoune, D. Bourissou, *Chem. Sci.* 2017, 8, 4539-4545. (d) J. Serra, P. Font, E. D. Sosa Carrizo, S. Mallet-Ladeira, S. Massou, T. Parella, K. Miqueu, A. Amgoune, X. Ribas, D. Bourissou, *Chem. Sci.* 2018, 9, 3932-3940.
- [13] E. Langseth, A. Nova, E. A. Tråseth, F. Rise, S. Øien, R. H. Heyn, M. Tilset, *J. Am. Chem. Soc.* 2014, 136, 10104-10115.
- [14] (a) M. W. Johnson, S. W. Bagley, N. P. Mankad, R. G. Bergman, V. Mascitti, F. D. Toste, *Angew. Chem. Int. Ed.* 2014, 53, 4404-4407. (b) A. V. Zhukhovitskiy, I. J. Kobylanski, C.-Y. Wu, F. D. Toste, *J. Am. Chem. Soc.* 2018, 140, 466-474.
- [15] J. A. Cadge, P. J. Gates, J. F. Bower, C. A. Russell, *J. Am. Chem. Soc.* 2022, 144, 19719-19725. Also see the related report on gold-catalyzed alkoxy-carbonylation of aryl and vinyl iodides utilizing ligand-enabled Au(I)/Au(III) redox catalysis: *Angew. Chem. Int. Ed.* 2024, DOI: 10.1002/anie.202410794.
- [16] V. W. Bhoyare, E. D. Sosa Carrizo, C. C. Chintawar, V. Gandon, N. T. Patil, *J. Am. Chem. Soc.* 2023, 145, 8810-8816.
- (17) W. Wang, M. Ding, C.-G. Zhao, S. Chen, C. Zhu, J. Han, W. Li, J. Xie, *Angew. Chem. Int. Ed.* 2023, 62, e202304019.
- [18] Deposition number 2348455 (for 3ae) and 2348456 (for 3as) contains the supplementary crystallographic data for this paper. The data is provided free of charge by the joint Cambridge Crystallographic Data Centre and Fachinformationszentrum Karlsruhe Access Structures service.
- [19] Selected reviews: (a) A. Borissow, Y. K. Maurya, L. Moshniaha, W.-S. Wong, M. Żyła-Karwowska, M. Stepień, *Chem. Rev.* 2022, 122, 565-788. (b) Q. Li, Y. Zhang, Z. Xie, Y. Zhen, W. Hu, H. Dong, *J. Mater. Chem. C* 2022, 10, 2411-2430.
- [20] (a) M. Rigoulet, O. T. du Boullay, A. Amgoune, D. Bourissou, *Angew. Chem. Int. Ed.* 2020, 59, 16625-16630. (b) C. C. Chintawar, A. K. Yadav, N. T. Patil, *Angew. Chem. Int. Ed.* 2020, 59, 11808-11813.
- [21] L. Huang, M. Rudolph, F. Rominger, A. S. K. Hashmi, *Angew. Chem. Int. Ed.* 2016, 55, 4808-4813.
- (22) For additional details, see the Supporting Information.
- [23] R. C. Larock, M. J. Doty, Q. Tian, J. M. Zenner, *J. Org. Chem.* 1997, 62, 7536-7537.
- [24] (a) G. J. Sherborne, A. G. Gevondian, I. Funes-Ardoiz, A. Dahiya, C. Fricke, F. Schoenebeck, *Angew. Chem. Int. Ed.* 2020, 59, 15543-15548. (b) J. Xie, K. Sekine, S. Witzel, P. Kramer, M. Rudolph, F. Rominger, A. S. K. Hashmi, *Angew. Chem. Int. Ed.* 2018, 57, 16648-16653.